

ARTICLES

Structural Changes of Argon Hydrate under High Pressure

Hisako Hirai,^{*,†} Yukako Uchihara,[†] Yukiko Nishimura,[†] Taro Kawamura,[‡]
Yoshitaka Yamamoto,[‡] and Takehiko Yagi[§]

Institute of Geoscience, University of Tsukuba, Tsukuba, Ibaraki 305-8571, Japan, National Institute for Resources and Environment, Tsukuba, Ibaraki 305-8569, Japan, and Institute for Solid State Physics, Tokyo University, 5-1-5 Kashiwanoha, Kashiwa, Chiba 277-8581, Japan

Received: June 19, 2002; In Final Form: August 7, 2002

Structural changes of argon hydrate were investigated in a pressure range of 0.2 to 6.5 GPa at room temperature using a diamond anvil cell. In-situ X-ray diffractometry and optical microscopy revealed a sequence of three different structures in this pressure–temperature range. Argon hydrate exhibited a well-known cubic structure II at the pressure range of 0.2 to 0.6 GPa. At 0.7 GPa the cubic structure II transformed into a tetragonal phase. At 1.1 GPa, the tetragonal phase further transformed into a body-centered orthorhombic phase, which survived pressures up to 6.0 GPa. At pressures higher than 6.1 GPa, the orthorhombic phase decomposed into solid argon and ice VII. Structural analysis showed that the tetragonal structure observed was composed of two 14-hedra occupying two argon atoms in a unit cell, which was very similar to the tetragonal structure reported in previous literature. The body-centered orthorhombic structure observed was explained as a “filled-ice” structure, a newly reported structure in a water–methane system at high pressure. These results showed that the cubic structure II of argon hydrate was transformed, by way of a tetragonal cage structure, into just such a “filled-ice” structure.

Introduction

Clathrate hydrates consist of cages formed by host water molecules, with guest molecules or atoms included in the cages. Numerous numbers of clathrate hydrates are known at present; comprehensive studies have been performed on various standing points such as phase relation,^{1,2} crystal structure,^{3–8} and physical property.^{6,9} Most clathrate hydrates show either cubic structure I (cs-I)³ or cubic structure II (cs-II),⁴ while some hydrates accommodating a larger guest molecule take a hexagonal structure (sH).^{5,7} It had been understood that the size of the guest molecule determines the selection among these structures. However, some hydrates containing small guest species such as Ar, N₂, and O₂ violate this selection rule; such clathrate hydrates select csII at ambient conditions. In addition, double occupancy of guests in the cage has been suggested for argon hydrate and N₂ hydrate under moderately higher pressures.^{10,11}

Pressure is one of the most important determinants of structural change, especially for clathrate structures consisting of cages. When a pressure effect is added to the formation of clathrate hydrates, it is expected that a different structure selection will occur or a completely new structure be formed. From this point of view, the present authors carried out a high-pressure study of methane hydrate and found three structures under high pressure.¹² Argon hydrate is unique in that the argon

atom is considered the smallest to be capable of forming a true clathrate structure.^{1,13} Considering their small size, spherical shape, and chemical inertness, argon atoms can be introduced into various types of cages, whether as single or double occupants, with a good possibility of structural changes occurring under conditions of high pressure.

High-pressure studies on argon hydrate have been carried out by several methods so far.^{14–17} Dyadin reported the presence of two high-pressure structures up to 1.5 GPa by determining the decomposition curves.¹⁴ Lozt also described two structures up to 3.0 GPa and 140 °C by a quasi-isochoric scanning method.¹⁵ These studies inferred that the structures observed at relatively lower pressure corresponded to cs-I, and that the one at the higher pressure was some denser hydrate, although structure analysis was not made. Manakov reported the presence of cs-II, sH, and a tetragonal structure up to 1.0 GPa,¹⁶ and Krunosov determined the tetragonal structure by a neutron diffraction study.¹⁷ These structural changes reported were not totally coincident. Discrepancies are probably due to kinetic conditions such as compression rate and the initial state of the sample. Further experiment is required to understand the behavior of argon hydrate at these pressure regions and higher regions.

In this study, in-situ X-ray diffractometry and optical microscopy were carried out on argon hydrate for pressures from 0.2 to 6.5 GPa at room temperature using a diamond anvil cell (DAC). Two high-pressure phases of argon hydrate were found: one having a primitive tetragonal structure and the other, a body-centered orthorhombic structure. Structural analysis was

* Author to whom correspondence should be addressed. Fax: +81-298-53-3990. E-mail: hhirai@sakura.cc.tsukuba.ac.jp.

[†] Institute of Geoscience, University of Tsukuba.

[‡] National Institute for Resources and Environment.

[§] Institute of Solid State Physics, Tokyo University.

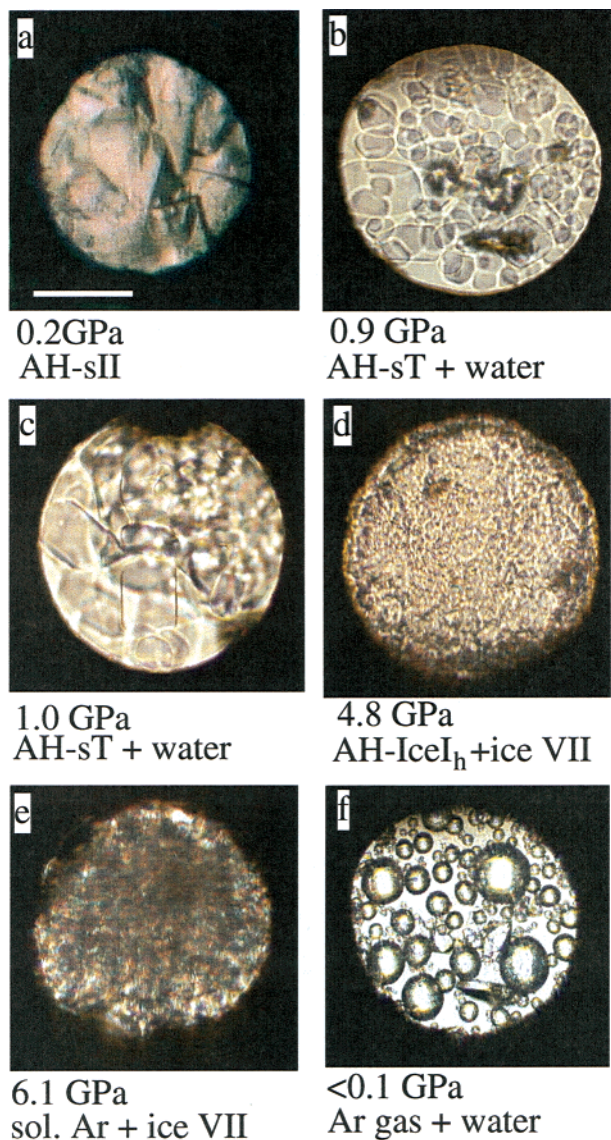


Figure 1. Optical micrographs showing phase changes with pressure. (a) at 0.2 GPa, (b) at 0.9 GPa, (c) 1.0 GPa, (d) at 4.8 GPa, (e) at 6.1 GPa, and (f) at <0.1 GPa. Scale bar is 100 μm .

performed on these phases. The high-pressure behavior of argon hydrate was compared with that of methane hydrate.

Experimental Section

A lever-and-spring type DAC was used in the high-pressure experiments. To control pressures lower than 2 GPa, several pairs of soft springs were used. Pressure measurements were made by the ruby fluorescence method. The accuracy of this measurement system is 0.1 GPa, taking both the resolutions of the spectrometer and the analytical procedure into account. The XRD experiment was performed using synchrotron radiation (SR) on BL-18C at Photon Factory, High Energy Accelerator Research Organization (KEK). A monochromatized beam with a wavelength of 0.09204 nm was used. The initial material was argon hydrate powder prepared using a conventional ice-gas interface method under the conditions of 11 MPa and $-2\text{ }^{\circ}\text{C}$. This powder consisted of almost pure argon hydrate according to a gas-chromatography analysis. The sample powder was put into a gasket hole in a vessel cooled by liquid nitrogen to prevent decomposition of the sample. The sample was sealed by loading the anvils to approximately 0.2 GPa at low temperature, and

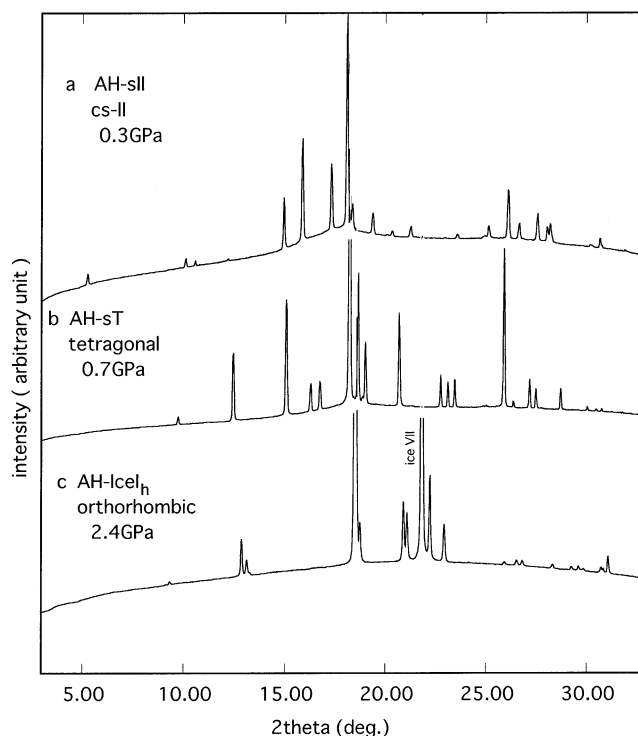


Figure 2. Representative X-ray diffraction patterns with pressure change. (a) AH-sII at 0.3 GPa, (b) AH-sT at 0.7 GPa, (c) AH-IceI_h at 2.4 GPa.

then the DAC was warmed to room temperature. The samples remained in a solid state during the procedures. The XRD study and optical observation were conducted at room temperature. The mean compression rate was approximately 0.1 GPa per 10 min.

Results

The starting material of argon hydrate represented fine powder, but crystal growth was observed after several hours (Figure 1a). The powder samples showed a typical XRD pattern of cs-II at 0.3 GPa (Figure 2a) (Table 1). In this paper, the argon hydrate showing cs-II is called AH-sII. At pressures of 0.2 to 0.6 GPa, the XRD pattern and the features of the AH-sII were unchanged. At 0.7 GPa, a vast number of brown spots and patches emerged in the AH-sII crystals. Simultaneously, rectangular crystals began to appear in the colorless fluid, possibly water. At this time, a new XRD pattern developed (Figure 2b). The diffraction lines observed were indexed as a tetragonal structure (Table 1). This phase of argon hydrate, called AH-sT in this study, was maintained from 0.7 to 1.0 GPa and coexisted with the colorless fluid, possibly water (Figure 1b,c).

At the pressure of 1.1 GPa, another new phase of argon hydrate was observed together with ice VI. At 2.1 GPa, the ice VI transformed into ice VII, and the new phase was unchanged. The XRD pattern of the new phase, called AH-IceI_h in this study, was indexed as a body-centered orthorhombic structure (Table 1). The AH-IceI_h survived up to 6.0 GPa (Figure 1d) (Figure 2c). Solid argon was not observed in this pressure range. At higher than 6.1 GPa, the AH-IceI_h decomposed into ice VII and solid argon (Figure 1e). When pressure was decreased, the AH-IceI_h reverted to the tetragonal AH-sT at 1.0 GPa. At the pressure from 1.0 to 0.7 GPa, the AH-sT was observed. The AH-sII reappeared at 0.6 GPa, and persisted to 0.2 GPa. At 0.1 GPa, the AH-sII decomposed into argon gas and water (Figure 1f). These phases were observed with good reproducibility in the experiments.

TABLE 1: The Observed and Calculated d spacings of AH-sII, AH-sT, and AH-IceI_h

AH-sII			AH-sT			AH-IceI _h		
at 0.3GPa			at 0.9GPa			at 2.1GPa		
(h k l)	d -obs. (nm)	d -calc. (nm)	(h k l)	d -obs. (nm)	d -calc. (nm)	(h k l)	d -obs. (nm)	d -calc. (nm)
(1 1 1)	0.9832	0.9889	(0 0 2)	0.5299	0.5296	(0 1 1)	0.5624	0.5604
(3 1 1)	0.5166	0.5164	(1 1 1)	0.4136	0.4140	(1 1 0)	0.4065	0.4073
(4 2 2)	0.3493	0.3496	(1 1 2)	0.3427	0.3429	(0 2 0)	0.3999	0.3987
(3 3 3)	0.3295	0.3296	(2 0 0)	0.3177	0.3181	(0 0 2)	0.3944	0.3939
(4 4 0)	0.3030	0.3028	(1 0 3)	0.3085	0.3087	(1 2 1) (1 1 2)	0.2840	0.2845
(5 3 1)	0.2894	0.2895	(2 1 0)	0.2843	0.2845	(0 2 2)	0.2805	0.2802
(6 2 0)	0.2708	0.2708	(1 1 3)	0.2777	0.2777	(0 3 1)	0.2527	0.2518
(6 2 2)	0.2584	0.2582	(0 2 2)	0.2725	0.2727	(0 1 3)	0.2496	0.2494
(4 4 4)	0.2470	0.2472	(2 1 2)	0.2504	0.2506	(2 0 0)	0.2372	0.2369
(5 5 1)	0.2398	0.2398	(2 2 0)	0.2248	0.2249	(1 3 0)	0.2304	0.2318
(5 5 3)	0.2229	0.2230	(2 1 3)	0.2214	0.2215	(2 2 0)	0.2041	0.2038
(7 3 3)	0.2093	0.2092	(1 0 5)	0.2011	0.2010	(2 0 2)	0.2033	0.2031
(6 6 0)	0.2020	0.2019	(2 2 3)	0.1897	0.1897	(1 3 2)	0.1994	0.1998
(5 5 5)	0.1977	0.1978	(3 0 3)	0.1818	0.1818	(1 2 3)	0.1990	0.1990
(8 4 0)	0.1915	0.1915	(3 2 3)	0.1578	0.1578	(0 0 4)	0.1971	0.1970
(7 5 3)	0.1879	0.1880	(4 1 0)	0.1544	0.1543	(0 3 3)	0.1870	0.1868
(8 4 4)	0.1747	0.1748	(3 3 0)	0.1500	0.1499	(2 2 2)	0.1810	0.1809
(7 5 5)	0.1722	0.1721	(3 3 1)	0.1482	0.1485	(1 4 1)	0.1792	0.1789
(7 7 3)	0.1652	0.1652	(3 3 2)	0.1442	0.1443	(0 4 2)	0.1778	0.1779
						(1 1 4)	0.1771	0.1773
						(2 3 1)	0.1726	0.1726
						(2 1 3)	0.1718	0.1718

 $a = 1.7128$ nm $a = 0.6362$ nm
 $c = 1.0592$ nm $a = 0.4742$ nm
 $b = 0.7973$ nm
 $c = 0.7878$ nm

Discussion

The present in-situ observation of XRD and optical microscopy revealed that three phases of argon hydrate, the cubic structure II (AH-sII), the primitive tetragonal structure (AH-sT), and the orthorhombic structure (AH-IceI_h), existed in sequence of increasing pressures up to 6.0 GPa. These three phases were observed reversibly both in increasing and decreasing pressure at room temperature. In the previous studies,^{14,15} a high-pressure phase observed in the range of 0.77 GPa to 0.95 GPa was inferred to be cubic structure I (cs-I), although an X-ray study was not conducted. That phase is thought to be the tetragonal AH-sT in the present study. Hexagonal structure (sH) was reported in a pressure range 0.47 to 0.77 GPa,¹⁶ but sH was not observed in that pressure range within the present experiments. The discrepancy of the phases formed may be attributed to difference in the states of the initial materials and/or difference in temperature around room temperature.

The structures of the argon hydrate phases were examined by a Rietveld analysis using the RIETAN computer program. As for the AH-sII, evidence for double occupancy in the large cages was not evaluated for the XRD data obtained, although double occupancy was suggested by a molecular dynamics calculation in the moderately high-pressure region, >20 MPa.¹⁰

All diffraction lines of the AH-sT were indexed as primary tetragonal structure (space group: $P4_2/mnm$), with unit cell parameters of $a = 0.6362$ nm and $c = 1.0592$ nm at 0.9 GPa (Table 1). Kurnosov et al. also reported a tetragonal structure and determined the structure by a neutron diffraction study.¹⁷ According to them, the structure is composed of 14-hedra expressed as $[4^25^86^4]$,⁶ with two argon atoms occupying each 14-hedron. The described Ar–Ar distance, 0.326 nm, is smaller compared with the effective diameter of Ar atom. There might be some interaction between the host water molecules and Ar atoms which counterbalances repulsion between the Ar atoms, or there might be more appropriate positions for Ar atoms. In the present structural analysis, the two 14-hedra were assumed and the RIETAN program was used only to refine the cage occupancy. The cage occupancy calculated was slightly lower,

1.8, for the XRD pattern analyzed, indicating that most but not all of the cages were occupied by two argon atoms. Within a unit cell of AH-sT, there are 12 oxygen atoms and 4 argon atoms in the case of full (double) occupancy. Thus, the ratio of water molecules to argon atoms is 12:4, while the ratio for the AH-sII (cs-II) is $136:24 = 12:2.11$ in the case of full occupancy. This means that about a half of the water content has to be extracted at the transition from AH-sII to AH-sT. In the present optical microscopy, the AH-sT was observed together with water (Figure 1b,c). This optical observation is consistent with the structural analysis.

For the AH-IceI_h, the observed diffraction pattern was explained as a body-centered orthorhombic structure with unit cell parameters of $a = 0.4742$ nm, $b = 0.7973$ nm, and $c = 0.7878$ nm at 2.1 GPa (Table 1). A similar body-centered orthorhombic structure (named as MH-III¹⁸ and named as MH-IceI_h in this paper) was found for methane hydrate at pressures of 2 to 10 GPa.^{12,18,19} The structure, determined by Loveday using a neutron diffraction study,⁸ closely resembles that of ice I_h, and can be understood as an ice I_h-like structure whose channels are filled with methane molecules; hence, its designation as a “filled-ice” structure.⁸ The present structural analysis showed that the AH-IceI_h was consistent with a “filled-ice” structure. The unit cell parameters of the AH-IceI_h are slightly smaller than those of the MH-IceI_h by about 3% in average¹² at the same pressure; this difference in unit cell parameters can be attributed to the difference in size between methane molecules and argon atoms. And, the ratio of unit cell parameters, b/c , of AH-IceI_h was changed with pressure, which might be caused by interaction with the host water molecules forming the channels. The present study is the first finding that argon hydrate reaches a “filled-ice” structure as a final structure at high pressure.

The present experimental results and structural analysis of argon hydrate revealed that the initial structure, cs-II (AH-sII), transformed via the tetragonal caged-structure (AH-sT) finally into a “filled ice” structure (AH-IceI_h) under high pressure. In contrast, methane hydrate begins as a cs-I (MH-sI) transforms

via a hexagonal caged-structure (named as MH-sH) into the “filled-ice” structure (MH-IceI_h),^{12,18,19} although a different transition path; i.e., from a cs-I via cs-II to sH, was also reported.²⁰ That transition path might be caused by kinetic effect. It is certainly of interest that, under very high pressures, a same “filled-ice” structure is selected, despite the fact that their initial and intermediate structures show variety. The present study leads to an understanding on transition behavior of gas hydrate under high pressure, although further high-pressure studies are required for other gas hydrates having different guest size, shape, and chemical properties.

References and Notes

- (1) Sloan, E. D. *Clathrate Hydrates of Natural Gases*, 2nd ed; Marcel Dekker: New York, 1998.
- (2) Nakano, S.; Moritoki, M.; Ohgaki, K. *J. Chem. Eng. Data* **1999**, *44*, 254.
- (3) McMullan, R. K.; Jeffrey, G. A. *J. Chem. Phys.* **1965**, *42*, 2725.
- (4) Mak, T. C. W.; McMullan, R. K. *J. Chem. Phys.* **1965**, *42*, 2732.
- (5) Ripmeester, J. A.; Tse, J. S.; Ratcliffe, C. I.; Powell, B. M. *Nature* **1987**, *325*, 135.
- (6) Jeffrey, G. A. *Inclusion Compounds*; Atwood, J. L., Davis, J. E. D., MacNicol, D. D., Eds.; Academic: London, 1984; Vol. 1.
- (7) Udachin, K. A.; Ratcliffe, C. I.; Enright, G. D.; Ripmeester, L. A. *Supramol. Chem.* **1997**, *8*, 173.
- (8) Loveday, J. S.; Nemes, R. J.; Guthrie, M.; Klug, D. D.; Tse, J. S. *Phys. Rev. Lett.* **2001**, *87*, 215501-1.
- (9) Davidson, D. W. *Natural Gas Hydrates: Properties, Occurrence and Recovery*; Cox, J. L., Ed.; Butterworth: Boston, 1983.
- (10) Itoh, H.; Tse, J. S.; Kawamura, K. *J. Chem. Phys.* **2001**, *115*, 9414.
- (11) Kuhs, W. F.; Chazallon, B.; Radaelli, P. G.; Pauer, F. J. *Inclusion Phenom. Mol. Recognit. Chem.* **1997**, *19*, 65.
- (12) Hirai, H.; Uchihara, Y.; Fujihisa, H.; et al. *J. Chem. Phys.* **2001**, *115*, 7066.
- (13) Dyadin, Y. A.; Larionov, E. G.; Manakov, A. Y.; et al. *Mendelev Commun.* **1999**, 209.
- (14) Dyadin, Y. A.; Larionov, E. G.; Mirinski, D. S.; Mikina, T. V.; Starostina, L. I. *Mendelev Commun.* **1997**, 32.
- (15) Lotz, H. T.; Schouten, J. A. *J. Chem. Phys.* **1999**, *111*, 10242.
- (16) Manakov, A. Y.; Voronin, V. I.; Kurnosov, A. V.; et al. *Dokl. Phys. Chem.* **2001**, *378*, 148.
- (17) Kurnosov, A. V.; Manakov, A. Y.; Komarov, V. Y.; et al. *Dokl. Phys. Chem.* **2001**, *381*, 303.
- (18) Loveday, J. S.; Nemes, R. J.; Guthrie, M.; et al. *Nature* **2001**, *410*, 661.
- (19) Shimizu, H.; Kumazaki, T.; Kume, T.; Sasaki, S. *J. Phys. Chem.* **2002**, *106*, 30.
- (20) Chou, I.-M.; Sharma, A.; Burruss, R. C.; Goncharov, A. F.; Hemley, R. J.; Stern, L. A.; Kirby, S. H. *Proc. Natl. Acad. Sci.* **2000**, *97*, 13484.